Novel Synchronous Rectification Method for WPT Only by DC Current Sensor

Daisuke Shirasaki
Graduate School of Frontier Science
The University of Tokyo
Kashiwa, Chiba, Japan
shirasaki.daisuke19@ae.k.u-tokyo.ac.jp

Hiroshi Fujimoto
Graduate School of Frontier Science
The University of Tokyo
Kashiwa, Chiba, Japan
fujimoto@k.u-tokyo.ac.jp

***Abstract*—To achieve high efficiency rectification, one option is to use synchronous rectification instead of diode rectification. However, synchronous rectification requires an expensive AC current sensor. This is one of the barriers when introducing synchronous rectification. Here we introduce a new synchronous rectification method that does not need any expensive AC current sensors. This new method just uses an DC current sensor, which is cheaper than AC current sensor. The principle of the method is explained in the first part, and the effect of the method is verified by experiments.**

Keywords—wireless power transfer, synchronous rectification, phase-shift power modulation

I. INTRODUCTION

In recent years, wireless power transfer (WPT) has become widely used in smartphones and other devices. Qi, which is used in smartphones, adopts the electromagnetic induction type. This type is simple but has the disadvantage of not being able to deliver enough power in an environment with a large air gap [1].

Magnetic resonant coupling, which MIT published in 2007 has attracted a lot of attention because it can transfer large power with high efficiency. Furthermore, it has the characteristic that it maintains high efficiency even with a wide air gap or misalignment [2].

So the WPT which uses magnetic resonant coupling has been researched even in areas where the air gap is wide. One application is a wireless power supply to EVs [3]. EVs have been widely used in recent years, but they have not been fully accepted by society. This would be due to the shorter range, higher vehicle price, and longer charging time compared to gasoline vehicles [4] [5] [6].

These problems can be resolved by dynamic wireless power transfer (DWPT). Power can be transferred from the road side to vehicles by installing road side coils to intersections in cities and expressway, and installing vehicle side coils to EVs like Fig. 1 [7].

There are some problems in DWPT. Improving the efficiency of the WPT is an important research theme [8]. There

Fig. 1. The experimental vehicle for DWPT

are some points to be improved for the high efficiency of the WPT. One part to be improved is the rectifier. Rectifiers use diodes in general, but diodes lose a certain amount of energy during rectification due to their forward voltage. Synchronous rectification can reduce the loss because the voltage drop by the on-resistance is lower than that by diodes in general [9] [10]. The rectifier that performs synchronous rectification has the same structure as a full-bridge inverter [11][12][13]. The rectifier has an AC current sensor, and monitors the phase of the AC current. The timing of switching is controlled to sync the phase of voltage and current by feedback. However, AC current sensor which can measure 85 kHz with small phase delay is expensive, and this increases the cost of the synchronous rectification.

So we propose a new method that does not need any AC current sensors in this paper. This method only needs a DC current sensor, which is cheaper than AC current sensor. The controller of the vehicle side inverter monitors the DC current of the vehicle side battery, and adjusts the timing of the vehicle side inverter so that the receiving DC current is maximized. As the result, the vehicle side settles into the synchronous rectification state.

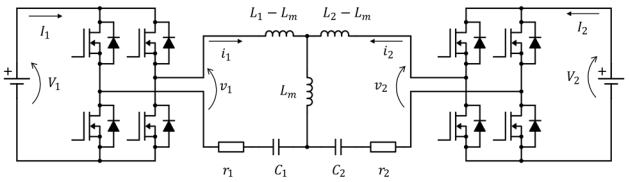

Fig. 2. S-S type resonance circuit

Chapter 2 introduces the principle of the proposed method. Then, Chapter 3 introduces how the proposed method realizes the synchronous rectification without AC current sensor specifically. In this section, the problem of hard switching is also discussed. Chapter 4 verifies the effect of the proposed method in an experiment.

II. PRINCIPLE OF AC SENSORLESS SYNCHRONOUS RECTIFICATION

The Series-Series(S-S) type resonance circuit is represented as shown in Fig. 2. The positive direction of the vehicle side current is defined as the direction of power transfer for the symmetry of the circuit. The resonance circuit is a bandpass-filter, so only the fundamental wave is considered.

The road side complex AC voltage $\dot{v_1}$ is described as the following equation by using the road side DC voltageV_1.

$$\dot{v_1} = \frac{4}{\pi\sqrt{2}}V_1 \tag{1}$$

The vehicle side complex AC voltage $\dot{v_2}$ is described as following equition by using V_2 and the phase lead of v_2 relative to v_1, θ.

$$\dot{v_2} = \frac{4}{\pi\sqrt{2}}V_2(\cos\theta + j\sin\theta) \tag{2}$$

In the resonant condition, the road side complex AC current $\dot{i_1}$ and the vehicle side complex AC current $\dot{i_2}$ are described as the following equations.

$$\dot{i_1} = \frac{r_2\dot{v_1} - j\omega L_m\dot{v_2}}{r_1r_2+\omega^2L_m^2} \tag{3}$$

$$\dot{i_2} = \frac{r_1\dot{v_2} - j\omega L_m\dot{v_1}}{r_1r_2+\omega^2L_m^2} \tag{4}$$

The vehicle side effective power P_2 and the vehicle side DC current I_2 are described as following equations.

$$P_2 = Re(\dot{v_2}\bar{i_2}) \tag{5}$$

$$I_2 = \frac{P_2}{V_2} \tag{6}$$

When the synchronous rectification works correctly, v_2 and i_2 are in opposite phases. Then, the phase of v_2 is advanced by 90° compared to the phase of v_1 as described in the phaser diagram Fig. 3.

TABLE I. MEANING AND VALUES OF THE PARAMETERS OF THE COILS

Parameter	Meaning	Value
V_1	DC Voltage of road side power-supply	15V
V_2	DC Voltage of vehicle side battery	15V
I_1	DC Current of road side	
I_2	DC Current of vehicle side	
v_1	AC Voltage of road side	
v_2	AC Voltage of vehicle side	
i_1	AC Current of road side	
i_2	AC Current of vehicle side	
C_1	Capacitance of road side coil	14.1 nF
C_2	Capacitance of vehicle side coil	34.5 nF
r_1	Resistance of road side coil	97.3mΩ
r_2	Resistance of vehicle side coil	28.1mΩ
L_1	Inductance of road side coil	24.8mH
L_2	Inductance of vehicle side coil	10.1mH
L_m	Mutual inductance	234.9mH
k	Coupling coefficient	0.148

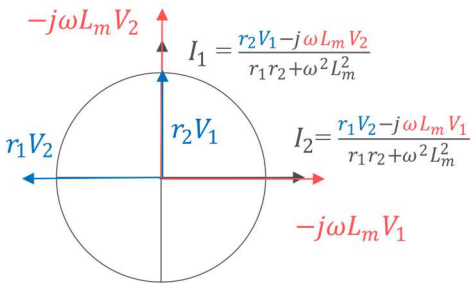

Fig. 3. The phase relationship of v_1, v_2, i_1, and i_2

Fig. 4 shows the relation between θ and the vehicle side received DC current $-I_2$ for various coupling coefficient k. Fig. 5 shows $-\frac{\partial I_2}{\partial\theta}$ for each θ and k. According to Fig. 5, $-\frac{\partial I_2}{\partial\theta}$ is positive when the θ is between $-90°$ and $90°$ for all k. This means that θ increases when the vehicle side controls the θ as to increases the received current $-I_2$. As the result, θ reaches $90°$ in the end. For all other values of θ, $-\frac{\partial I_2}{\partial\theta}$ is negative for all k. This means that θ decreases when the vehicle side controls the θ as to increases the received current $-I_2$. As the result, θ reaches $90°$ in the end. So, for all θ and k, the θ reaches $90°$ when the vehicle side controls the θ as to increases the received current $-I_2$. Fig. 8 shows the relation between θ and $-I_2$ when $k = 0.148$. (k has a maximum value of 0.148 at the center of the coil.) This figure also shows that the vehicle side received DC current $-I_2$ reaches at its maximum when the θ is 90°.

III. METHOD OF AC SENSORLESS SYNCHRONOUS RECTIFICATION

From this analysis, a novel method of synchronous rectification is derived.

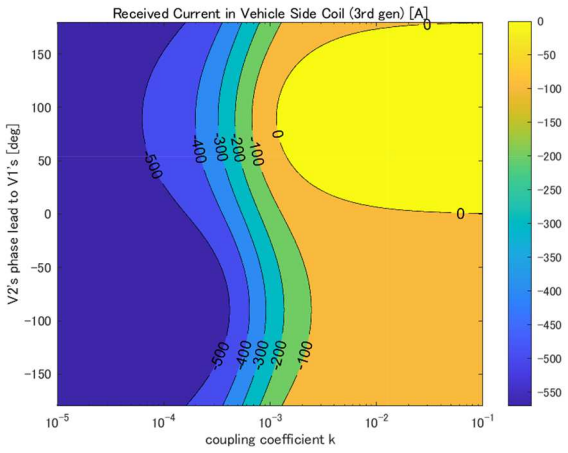

Fig. 4. The color map showing the relationship of θ, k, and $-I_2$

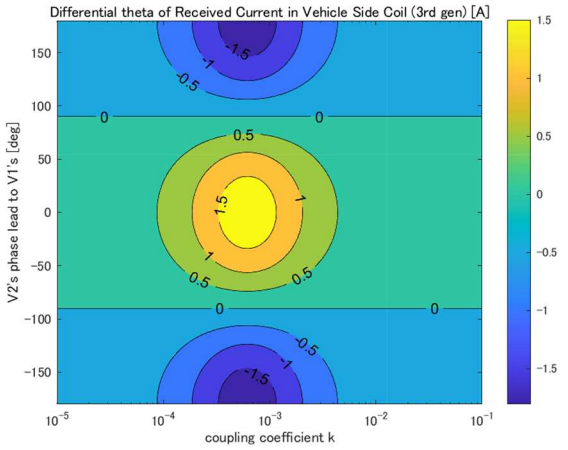

Fig. 5. The color map showing the relationship of θ, k, and $-\frac{\partial I_2}{\partial \theta}$

The road side just transfers power. The vehicle side changes θ while monitoring the vehicle side DC current. The road side and the vehicle side are offline, so the vehicle side cannot get the value of θ, but it can change θ by adjusting the timing of the vehicle side inverter.

The θ when the vehicle side receives maximum current is the θ when the synchronous rectification works correctly as explained in the previous chapter, so the vehicle side changes θ in the direction where the vehicle side DC current becomes larger. The control algorithm of θ is shown in Fig. 6.

The first θ is not a specific value because the vehicle side inverter and the road side inverter are not connected or synchronized. So, the vehicle side inverter cannot measures θ. However, the vehicle side inverter can adjust θ by changing the amount of delay of the switching timing, assuming that the road side operating without change.

At the beginning of the algorithm, the vehicle side inverter memories the current θ (= current amount of delay) as θ_{ref} and the I_2 as I_{ref}. Then, the vehicle side inverter increases θ by

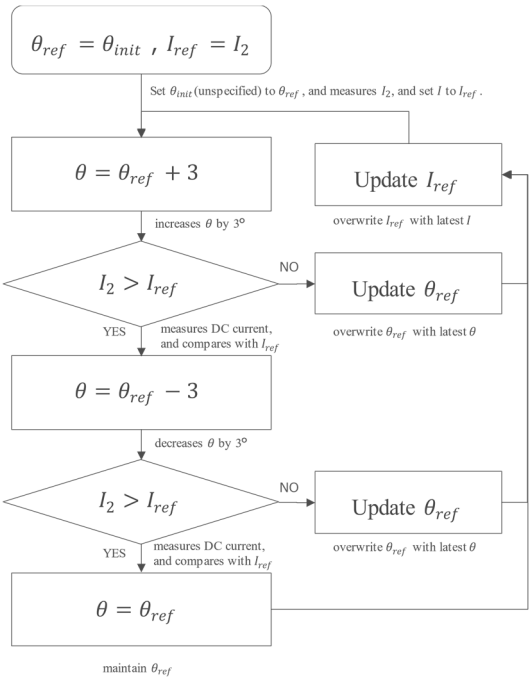

Fig. 6. The control algorithm of θ

adjusting the amount of the delay for switching, and measures I_2. If the I_2 is lower than I_{ref} , θ_{ref} is updated with current θ, and I_{ref} is also updated with current I_2. If I_2 is higher than I_{ref} , θ is changed to $\theta_{ref} - 3°$, and the same is done.

The road side and vehicle side is offline, so the vehicle side inverter cannot know θ is increased or decreased when it changes the amount of delay. However, the important point is that θ can be adjusted into both direction, and it is not important whether θ is increased or decreased first.

By repeating this algorithm, θ is adjusted so that I_2 is minimized. The value of 3° for the adjustment range was determined empirically.

A. About Switching Loss

When the θ is not 90°, the phase difference between v_2 and i_2 is not 0°. So the hard switching happens in the situation. In that situation, the received current $-I_2$ decreases compared to the ideal switching situation due to the switching loss. The switching loss is calculated to assess whether it is significant for the phase control algorithm.

First, the current at switching timing i_{2SW} is calculated from $|i_2|$ and the phase difference between v_2 and i_2. Then, the switching loss energy [J/switching] is read from the graph in the datasheet of the SiC used in the inverter (SCH2080KE) [14]. Fig. 7 shows the relationship between the drain current and the switching loss per switching. The value from 0A to 10A is extrapolated. The switching loss energy read from the graph is the value when the V_{DD} is 600V, so it is corrected by the actual applied voltage. So the switching loss per second is described by Equ. 7. The meanings of each parameter are shown in Table II.

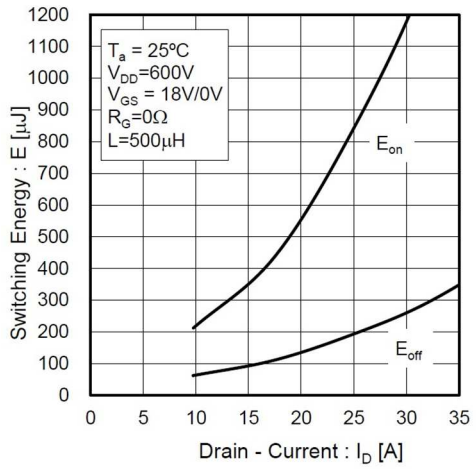

Fig. 7. The switching Loss of SCH2080KE

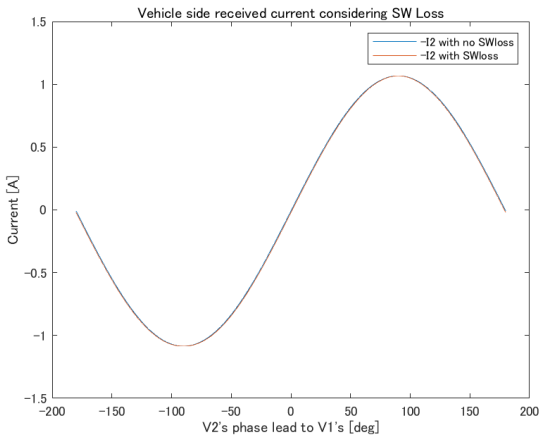

Fig. 8. The impact of SW Loss

$$P_{SWL} = \{P_{DSLon}(i_{2SW}) + P_{DSLoff}(i_{2SW})\} \times \frac{\frac{v_2}{2}}{600} \times f \times 4 \quad (7)$$

Fig. 8 shows the relationship between θ and $-I_2$, and Fig. 9 is an enlargement of Fig. 8 for θ in the range of 50◦ to 130◦. The switching loss sharpens the curve of the graph a little compared to the ideal condition. This leads to increases the change of the current when the θ changes. As the result, the accuracy of the synchronous rectification improves. However, the effect is small, and the switching loss will not affect the accuracy of the synchronous rectification of the proposed method in real.

IV. ANALYSIS IN EXPERIMENT

The effect of the proposed method was verified in the experiment at a standstill. The vehicle side coil is fixed on the center of the road side coil. The coupling coefficient at that point is 0.148 as described in Table I.

In this experiment, both the road side and vehicle side inverters are connected to the same DSP (Myway PE-Expert4). So, the phase lead of v_2 relative to v_1, θ can be changed directly from the DSP.

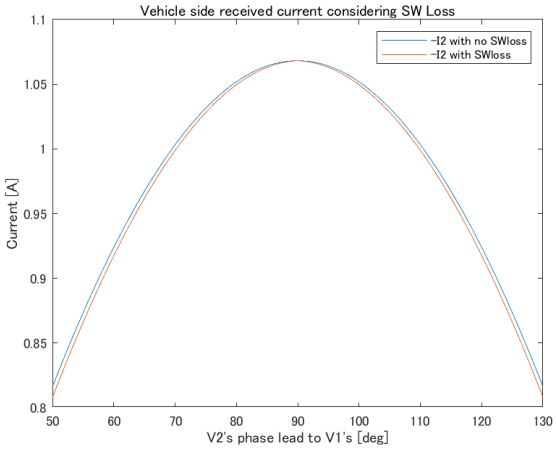

Fig. 9. The impact of SW Loss (Enlarged)

TABLE II. MEANING OF PARAMETERS OF THE CALCULATION OF SWITCHING LOSS

Parameter	Meaning	Unit
P_{SWL}	Switching loss	[W]
i_{2SW}	Vehicle side AC current when switching	[A]
$P_{DSL}(i)$	The raw switching loss value read from Fig. 7 when i flows	[J]
f	frequency of the inverter	[Hz]

The θ is set to 0° in the first condition. In this condition, the phase difference between v_2 and i_2 is not 0°, and hard switching is happening. The DSP monitors the I_2 only, and changes θ according to the algorithm in Fig. 6. Fig. 10 shows the result of the experiment. As the control algorithm starts at 0ms, the θ increases gradually by the algorithm, and the I_2 decreases. About 4ms after the algorithm started, the θ settled around 90°. In the final condition, the phase difference between v_2 and i_2 is almost 0°, and the synchronous rectification has been achieved as shown in Fig. 11.

V. CONCLUSION

In this paper, a novel synchronous rectification method without AC current sensors was proposed. The principle of how the method works is shown, and it is revealed that the impact of the switching loss on the proposed method is small enough to ignore. Then, the experiment in which the proposed method is implemented is conducted, and the effectiveness of the proposed method is demonstrated by the result that the vehicle side settles into the synchronous rectification state in short period.

VI. ACKNOWLEDGMENT

This work was partly supported by JST-Mirai Program Grant Number JPMJMI17EM, JSPS KAKENHI Grant Number JP18H03768, JST CREST Grant Number JPMJCR15K3, JSPS KAKENHI Grant Number 19H02123.

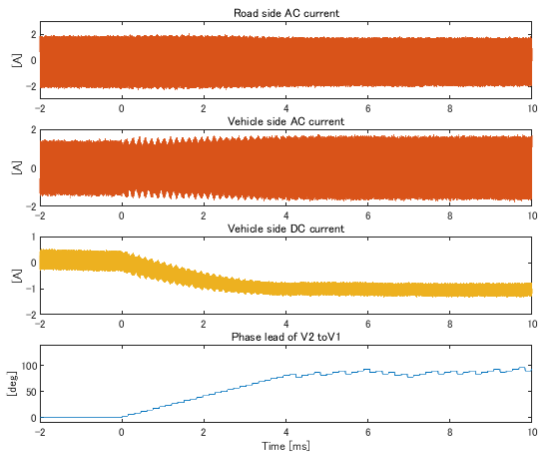

Fig. 10. The experimental waveform of the proposed control algorithm

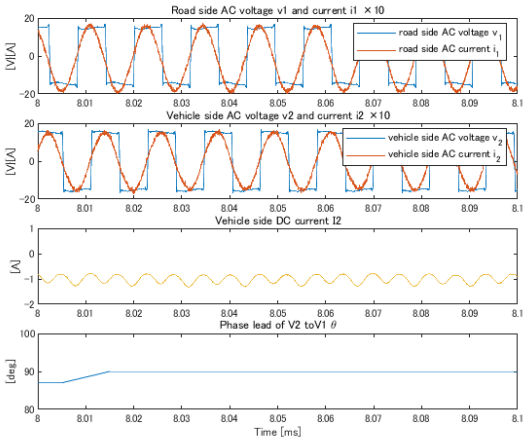

Fig. 11. The waveform after synchronous rectification

REFERENCES

[1] S. Y. Hui, “Planar wireless charging technology for portable electronic products and Qi,” Proceedings of the IEEE, vol. 101, no. 6, pp. 1290–1301, 2013.

[2] A. Kurs, A. Karalis, R. Moffatt, J. Joannopoulos, P. Fisher, and M. Soljacic, “Wireless power transfer via strongly coupled magnetic resonances.(RESEARCH ARTICLES)(Author abstract),” vol. 317, no. 5834, p. 83(4), 2007.

[3] F. Lu, H. Zhang, C. Zhu, L. Diao, M. Gong, W. Zhang, and C. C. Mi, “A Tightly Coupled Inductive Power Transfer System for Low-Voltage and High-Current Charging of Automatic Guided Vehicles,”IEEE Transactions on Industrial Electronics, vol. 66, no. 9, pp. 6867–6875, 2019.

[4] J. P. Sampath, D. M. Vilathgamuwa, and A. Alphones, “Efficiency Enhancement for Dynamic Wireless Power Transfer System with Segmented Transmitter Array,” IEEE Transactions on Transportation Electrification, vol. 2, no. 1, pp. 76–85, 2016.

[5] P. K. S. Jayathurathnage, A. Alphones, D. M. Vilathgamuwa, and A. Ong, “Optimum Transmitter Current Distribution for Dynamic Wireless Power Transfer with Segmented Array,” IEEE Transactions on Microwave Theory and Techniques, vol. 66, no. 1, pp. 346–356, 2018.

[6] I. S. Suh and J. Kim, “Electric vehicle on-road dynamic charging system with wireless power transfer technology,” Proceedings of the 2013 IEEE International Electric Machines and Drives Conference, IEMDC 2013, pp. 234–240, 2013.

[7] H. Fujimoto, O. Shimizu, S. Nagai, T. Fujita, D. Gunji, and Y. Ohmori, “Development of wireless in-wheel motors for dynamic charging: From 2nd to 3rd generation,” 2020 IEEE PELS Workshop on Emerging Technologies: Wireless Power Transfer, WoW 2020, pp. 56–61, 2020.

[8] A. Pevere, R. Petrella, C. C. Mi and Shijie Zhou, "Design of a high efficiency 22 kW wireless power transfer system for EVs fast contactless charging stations," 2014 IEEE International Electric Vehicle Conference (IEVC), 2014, pp. 1-7, doi: 10.1109/IEVC.2014.7056221.

[9] F. Liu, W. Lei, T. Wang, C. Nie, and Y. Wang, “A phase-shift softswitching control strategy for dual active wireless power transfer system,” 2017 IEEE Energy Conversion Congress and Exposition, ECCE 2017, vol. 2017-January, pp. 2573–2578, 2017.

[10] A. Konishi, K. Umetani, and E. Hiraki, “High-frequency Self-Driven Synchronous Rectifier Controller for WPT Systems,” 2018 International Power Electronics Conference, IPEC-Niigata - ECCE Asia 2018, pp. 1602–1609, 2018.

[11] D. Tajima, O. Shimizu, and H. Fujimoto, “High-Efficiency Operation of Wireless In-Wheel Motor at Low Load Using Intermittent Synchronous Rectification with Improved Transient Stability,” IECON Proceedings (Industrial Electronics Conference), vol. 2019-October, pp. 1089–1094, 2019.

[12] Giorgio Lovison, Takehiro Imura, Hiroshi Fujimoto, and Yoichi Hori, “Secondary-side-only Phase-shifting Voltage Stabilization Control with a Single Converter for WPT Systems with Constant Power Load,” IEEJ J. Industry Applications, vol. 8, no. 1, pp. 66--74, 2019.

[13] Duy-Dinh Nguyen, Duc Tuyen Nguyen, and Goro Fujita, “New Modulation Strategy Combining Phase Shift and Frequency Variation for Dual-Active-Bridge Converter”, IEEJ J. Industry Applications, vol. 6, no. 2, pp. 140--150, 2017.

[14] ROHM Semiconducter, “SCH2080KE: SiC Power Devices Datasheet,” 2018.